Pharm Res (2015) 32:275–285
DOI 10.1007/s11095-014-1461-9

RESEARCH PAPER

Semi-Interpenetrating Network (sIPN) Co-Electrospun Gelatin/Insulin Fiber Formulation for Transbuccal Insulin Delivery

Leyuan Xu • Natasha Sheybani • Shunlin Ren • Gary L. Bowlin • W. Andrew Yeudall • Hu Yang

Received: 3 March 2014 / Accepted: 2 July 2014 / Published online: 17 July 2014

ABSTRACT

Purpose This work was aimed at developing a semi-interpenetrating network (sIPN) co-electrospun gelatin/insulin fiber scaffold (GIF) formulation for transbuccal insulin delivery.

Methods Gelatin was electrospun into fibers and converted into an sIPN following eosin Y-initiated polymerization of polyethylene glycol diacrylate (PEG-DA). The cytocompatibility, degradation rate and mechanical properties were examined in the resulting sIPNs with various ratios of PEG-DA to eosin Y to find a suitable formulation for transbuccal drug delivery. Insulin was co-electrospun with gelatin into fibers and converted into an sIPN-GIF using this suitable formulation. The *in vitro* release kinetics of insulin was evaluated using ELISA. The bioactivity of released insulin was analyzed in 3T3-L1 preadipocytes using Western blotting and Oil Red O staining. The transbuccal permeability of released insulin was determined using an *in vitro* porcine oral mucosa model.

Results The sIPN-GF formulation of GF cross-linked by PEG-DA (1% *w/v*) with eosin Y (5% *v/v*) possessed no cytotoxic effect, a moderate degradation rate with degradation half-life of 49 min, and a significant enhancement in mechanical properties. This formulation was used to fabricate sIPN-GIF. Insulin release was extended up to 4 h by sIPN-GIF. The released insulin successfully triggered intracellular AKT phosphorylation and induced adipocyte differentiation in 3T3-L1 preadipocytes. The transbuccal permeability of released insulin was determined on the order of 10^{-7} cm/s.

Conclusions Insulin can be fabricated into an sIPN-GIF formulation following co-electrospinning and cross-linking without losing bioactivity. It proved the potential of this new formulation for transbuccal insulin delivery.

KEY WORDS electrospun gelatin fiber · insulin · semi-interpenetrating network · transbuccal delivery

L. Xu (✉) · N. Sheybani · H. Yang (✉)
Department of Biomedical Engineering, Virginia Commonwealth University, 401 West Main Street, P.O. Box 843067 Richmond Virginia 23284, USA
e-mail: lxu3@vcu.edu
e-mail: hyang2@vcu.edu

S. Ren
Department of Internal Medicine, Virginia Commonwealth University/ McGuire Veterans Affairs Medical Center, Richmond Virginia 23249, USA

G. L. Bowlin
Department of Biomedical Engineering, University of Memphis, Memphis, Tennessee 38152, USA

W. A. Yeudall
Philips Institute of Oral and Craniofacial Molecular Biology, Virginia Commonwealth University, Richmond, Virginia 23298, USA

H. Yang
Massey Cancer Center, Virginia Commonwealth University, Richmond Virginia 23298, USA

ABBREVIATIONS

GF	Electrospun gelatin fiber scaffold
GI tract	Gastrointestinal tract
GIF	Co-electrospun gelatin/insulin fiber scaffold
PEG-DA	Polyethylene glycol diacrylate
sIPN	Semi-interpenetrating network scaffold
sIPN-GF	Semi-interpenetrating network electrospun gelatin fiber scaffold
sIPN-GIF	Semi-interpenetrating network co-electrospun gelatin/insulin fiber scaffold

INTRODUCTION

Diabetes mellitus is a group of metabolic diseases characterized by hyperglycemia as a result of lack of insulin production or response [1]. It is the seventh leading cause of death in the U.S. About 8.3% of the U.S. population had diabetes in 2011.

It was projected that one of three U.S. adults would develop diabetes by 2050 following the current trend [2]. Diabetes management relies on insulin administration. The primary route of administration for insulin is subcutaneous injection, which, however, is commonly associated with poor patient compliance and side effects such as the risk of hypoglycemia [1, 3]. Therefore, there is an imperative need to explore alternative routes of administration and develop non-invasive formulations for efficient delivery and patient compliance improvement.

So far, non-invasive oral, nasal, buccal, transdermal, rectal, and ocular delivery methods have been investigated [4, 5]. Oral insulin delivery is considered the most patient-friendly route [3]. However, the oral bioavailability of insulin is severely limited by its inherent structural susceptibility and low permeability across biological membranes in the gastrointestinal (GI) tract [6]. A variety of oral delivery systems have been developed based on natural polymers (*e.g.*, chitosan) and biocompatible biodegradable synthetic polymers (*e.g.*, poly(lactide-co-glycolide), PLGA) [7–10] to protect insulin from acidic and enzymatic gradation in the GI tract or enhance its intestinal absorption. Nonetheless, insulin oral bioavailability is still low, generally less than 10% [7, 8, 11–14]. Transbuccal delivery appears to be another compelling alternative to subcutaneous injection because it allows insulin to enter the systemic circulation by bypassing the first-pass effect and avoiding GI tract degradation, thus improving insulin bioavailability [15]. Furthermore, the transbuccal route can bring about a stable blood drug concentration with rapid onset [16]. Mucoadhesive formulations such as insulin-loaded Pluronic F-127 hydrogels [17], insulin-loaded PEG-*b*-PLA nanoparticles embedded chitosan films [18, 19], insulin-loaded chitosan-ethylenediaminetetracetic acid (chitosan-EDTA) films [20–22], have been applied to deliver insulin across the buccal mucosa.

Electrospun fibers have been actively utilized in tissue engineering owing to high surface area to volume ratios and well controlled structures and properties [15, 23]. We recently developed semi-interpenetrating electrospun gelatin fiber scaffolds (sIPNs) using polyethylene glycol diacrylate (PEG-DA) as a cross-linker [24]. The fiber structures, mechanical properties, degradation and drug release kinetics can be controlled by modulating the concentration of the cross-linker. Small-molecular-weight antifungal drugs, *e.g.*, nystatin, can be incorporated into the fiber construct during electrospinning [24]. An advantage of using PEG-DA as cross-linker is that cross-linking reaction only takes place between PEG-DA chains, leaving incorporated therapeutics intact. This strategy could be particularly useful for delivery of biological molecules such as insulin. However, the challenge of using sIPN-GF to deliver insulin is to ensure the insulin remains bioactive through the electrospinning and cross-linking process. In this work, we report a new buccal formulation, namely semi-interpenetrating network co-electrospun gelatin/insulin fiber formulation (sIPN-GIF), for insulin delivery. We particularly addressed two fundamental questions: 1) whether or not insulin can retain its activity following co-electrospinning and cross-linking; and 2) whether or not insulin can be released from the formulation and cross the buccal mucosa. Particularly, we examined AKT phosphorylation and adipocyte differentiation of 3T3-L1 preadipocytes treated with released insulin. The transbuccal permeability of insulin released from sIPN-GIF was evaluated using an *ex vivo* porcine oral mucosa model.

MATERIALS AND METHODS

Materials

1-vinyl-2 pyrrolidinone (NVP), eosin Y, ethanol, oil red O, phosphate buffer saline (PBS), polyethylene glycol diacrylate (M_n=575 g/mol; PEG-DA), gelatin from porcine skin (gel strength 300, type A), triethanolamine (TEOA), human recombinant insulin (meets USP testing specifications), dexamethasone (DEX), and 3-isobutyl-1-methylxanthine (IBMX) were purchased from Sigma-Aldrich (St. Louis, MO). 1,1,1,3,3,3-hexafluoro-2-propanol (HFP) was purchased from TCI America (Portland, OR). Cell proliferation reagent WST-1 was purchased from Roche Applied Science (Indianapolis, IN). Insulin enzyme-linked immunosorbent assay (ELISA) kit was purchased from Calbiotech (Spring Valley, CA). Phospho-AKT (Ser473) (p-AKT) antibody was purchased from Cell Signaling Technology (Danvers, MA). AKT1 (559028) antibody was purchased from BD Biosciences Pharmingen (Mississauga, ON, Canada). β-actin (ACTBD11B7) antibody was purchased from Santa Cruz Biotechnology (Santa Cruz, CA). Goat anti-rabbit antibody conjugated to horseradish peroxidase, goat anti-mouse antibody conjugated to horseradish peroxidase, and polyvinylidene difluoride (PVDF) were purchased from Bio-Rad (Hercules, CA). Dulbecco's modified Eagle's medium (DMEM) was purchased from Life Technologies (Grand Island, NY). Fetal bovine serum (FBS) was purchased from Fisher Scientific (Pittsburgh, PA). Penicillin and streptomycin were purchased from Thermo Fisher Scientific (Ashville, NC). Pierce ECL Western blotting substrate chemiluminescence was purchased from Thermo Scientific (Rockford, IL). Franz diffusion cell was purchased from PermeGear (Hellertown, PA).

Cell Culture

3T3-L1 preadipocytes were maintained in DMEM supplemented with high glucose, L-glutamine, FBS (10% *v*/*v*), penicillin (100 units/ml) and streptomycin (100 μg/ml) at 37°C in a humid environment with 5% CO_2.

Preparation of GFs

Electrospinning solutions were prepared first. Briefly, 1 g of gelatin alone or with 5 mg of insulin was dissolved in 10 ml of HFP, and the solution was shaken continuously overnight to obtain a homogeneous solution. To fabricate electrospun GFs or GIFs, a syringe containing gelatin solution or gelatin/insulin solution was placed in an electrostatic field, and 25 kV was applied to a blunt needle (18 gauge, 1.5 in. length). A grounded flat stainless steel collecting mandrel (7.5×2.5×0.5 cm, length × width × thickness) was placed 12.5 cm away from the needle. The electrospinning solution was dispensed from the syringe into the electrostatic field at a rate of 6.37 ml/h. The electrospun fibers deposited on the collecting mandrel with a rotational speed of 550 rpm and a translational speed of 6 cm/s over 12 cm were collected.

Preparation of sIPN-GFs and GIFs

An eosin Y-based photoinitiating system solution was composed of eosin Y (0.1% *w/v*), TEOA (40% *w/v*) and NVP (4% *w/v*) in ethanol [25]. Serial cross-linking solutions were prepared by combining various amounts of PEG-DA and eosin Y-based photoinitiating system. Cross-linking solution was then poured onto a piece of GF or GIF (600 μl of cross-linking solution per 200 mg of scaffold). They were exposed to ultraviolet (UV) light (100 W UVP Blak-Ray Long Wave Lamp) at a distance of 14 cm for 5 min on each side of the scaffold and then air-dried (Table I).

Cytocompatibility Assay

To evaluate the cytocompatibility of PEG-DA, a PEG-DA ethanol stock solution (500 mM) was prepared first. 3T3-L1 preadipocytes were incubated with final concentrations of PEG-DA (0–1,000 μM) in culture media for 2 days, and then cell viability relative to untreated cells was determined by WST-1 proliferation assay (n=5). Its half maximal inhibitory concentration (IC_{50}) was determined by using GraphPad Prism 5.

An elution method was applied to evaluate the cytocompatibility of the fabricated scaffolds [26]. Briefly, scaffold (20 mg) was immersed into 5 ml of cell culture medium at 37°C for 2 h. The elution medium was then collected and used to treat 3T3-L1 preadipocytes for 2 days. At the end of treatment, cell viability was determined by using WST-1 proliferation assay (n=5).

Table I GF and sIPN-GF formulations: 200 mg of GF was cross-linked with 600 μl of cross-linking solution, which contained PEG-DA and eosin Y photoinitiator solution

Scaffold	PEG-DA (*w/v*)	Eosin Y photoinitiator solution (*v/v*)
GF1	0%	0%
GF2	0%	5%
GF3	1%	0%
sIPN-GF1	1%	5%
sIPN-GF2	2%	5%
sIPN-GF3	5%	5%
sIPN-GF4	10%	5%
sIPN-GF5	1%	2%
sIPN-GF6	1%	10%

In Vitro Degradation Studies

In vitro degradation of the fabricated scaffolds in DMEM was evaluated. Scaffolds (20 mg each) were incubated in DMEM at 37°C for various lengths of time (15, 30, 60 and 120 min). At the pre-determined time intervals, the remaining scaffolds were collected. Small pieces of insoluble scaffolds were collected following centrifugal removal of DMEM medium. The combined residual scaffolds were lyophilized and weighed (n=5). Three different mathematical models were applied to fit the data, including first order polynomial model, second order polynomial model, and one phase decay model. To determine a model that best fits experimental data, fitting models were compared by running Akaike information criterion (AIC) test. Models with lower AIC values are more likely to be correct. One phase decay model was found to best describe the data. Degradation half-life ($t_{1/2}$), defined as time required for 50% scaffold mass loss, was determined by using GraphPad Prism 5, and degradation rate constant (K_d) was calculated as $K_d=\ln 2/t_{1/2}$.

Uniaxial Tensile Testing

Uniaxial tensile testing of electrospun scaffolds was performed as previously described [27]. Dog-bone-shaped samples (n= 12–18) were cut out using a punch die (ODC Testing & Molds) with a dimension of 19.05 mm in length, 3.175 mm at narrowest point and 6.1 mm at widest point. Scaffold thickness was determined using a digital caliper. Mechanical properties of the samples were tested using an MTS Bionix 200 testing system with a 100 N load cell. Samples were tested to failure at a strain rate of 1.33 min^{-1}. TestWorks version 4 was used for data acquisition and analysis of peak load, peak stress, modulus, strain at break and energy to break.

Scanning Electron Microscopy (SEM)

Scaffolds (20 mg each) were incubated in DMEM at 37°C for various lengths of time, *i.e.*, 15, 30, 60 and 120 min. Following removal of the incubation media by centrifugation at 6,000 g for 5 min, the residual scaffolds were collected and lyophilized. Each dried sample or GF, sIPN-GF1 was mounted on an

aluminum stub and sputter-coated with gold for 1 min. SEM images of scaffolds were taken on a JEOL LV-5610 scanning electron microscope at 20 kV. The diameters of 60 randomly chosen fibers per image were determined by using NIH ImageJ [27].

Insulin Release Studies

Insulin-loaded scaffolds (20 mg each) were incubated in 5 ml of DMEM at 37°C. At the pre-determined time points (15, 30, 60, 120 and 240 min), an aliquot (25 μl) was withdrawn and analyzed with ELISA for insulin quantification. Cumulative release of insulin from the scaffolds was then determined.

AKT Activation Analysis

To evaluate the bioactivity of released insulin in each sample, 3T3-L1 preadipocytes were used as a model. 20 mg of each fabricated scaffold (GF1, sIPN-GF1 and GIF) was incubated in 5 ml of cell culture media for 30 min, while 20 mg of sIPN-GIF was incubated in 5 ml of cell culture media for 15, 30, 60 and 120 min. Pre-seeded 3T3-L1 preadipocytes were then treated with 2 ml of insulin released media or free insulin (10 μg/mL) for 10 min. Activation of AKT in response to released insulin treatment was analyzed by Western blotting with the antibodies that recognizes phosphorylated-AKT at serine-473 (p-AKT) and total AKT (AKT1). Western blotting of total cellular protein was carried out by standard procedures [28]. The total cellular expression of β-actin was used as the loading control.

Oil Red O Staining

According to the standard protocol [29, 30], an induction medium was DMEM supplemented with FBS (10% *v/v*), DEX (10 μg/ml), IBMX (0.5 mM) and insulin (10 μg/ml), while an insulin medium was DMEM supplemented with FBS (10% *v/v*) and insulin (10 μg/ml). In this experiment, insulin release medium was obtained by incubating sIPN-GIF in DMEM for 2 h and then supplemented with FBS (10% *v/v*). The induction insulin release medium was the insulin release medium further supplemented with DEX (10 μg/ml) and IBMX (0.5 mM).

The differentiation was initiated by incubating the cells in the induction medium or induction insulin release medium for 2 days. At the end of day 2, the induction media were replaced with insulin medium or insulin release medium, and the cells were cultured for 2 days. At the end of day 4, the insulin media were replaced with DMEM containing with FBS (10% *v/v*) and refreshed the media every other day. At Day 10, the cells were rinsed in PBS three times and then fixed with formaldehyde (10% *w/v*) for 2 h. The cells were washed with PBS for three times, immersed in isopropanol (60% *v/v*) for 2 min, and then stained with Oil Red O (0.2% *w/v*) for 10 min. The cells were washed with PBS for three times and then imaged under a light microscope equipped with an image recorder.

In Vitro Permeation Studies

Fresh porcine cheek tissues were obtained from Silver Ridge Slaughter House (Fredericksburg, VA). Excesses of connective and adipose tissues were trimmed off to obtain a thickness of approximately 0.6 ± 0.1 mm as measured by a digital caliper. The transbuccal permeability of insulin released from sIPN-GIF was evaluated using the Franz diffusion cell model as previously described [31].

The permeation experiments were carried out using PBS in the receiver chamber and simulated saliva fluid (SSF; 12 mM KH_2PO_4, 40 mM NaCl, 1.5 mM $CaCl_2$, adjusted to pH 6.2 with NaOH) in the donor chamber to mimic the *in vivo* physiological conditions [24]. The sIPN-GIF (2.5 mg) was placed on the top of the mucosa membrane and immersed in 1 ml of SSF. At given time points up to 4 h, an aliquot of 1 ml from the receiver chamber was collected *via* syringe and analyzed by ELISA. Fresh PBS (1 ml) was added to the receiver chamber following each sampling. An equivalent amount of free insulin in SSF was used as a control. The permeability coefficient, P, was calculated as follows:

$$P = (dQ/dt)/AC$$

where dQ/dt is the steady-state slope of a cumulative flux curve, C is insulin concentration in the donor chamber, and A is the effective cross-sectional area (0.785 cm^2) available for diffusion [31]. The degradation of sIPN-GF1 was also monitored.

Statistical Analysis

Curve fitting was performed using GraphPad Prism 5 as nonlinear or linear regression. The data were expressed as means ± standard deviation (SD) and analyzed using one way analysis of variance (ANOVA) followed by Tukey's multiple comparison test for subgroup comparison. A value of $p<0.05$ was considered statistically significant.

RESULTS

Cytocompatibility of sIPN-GFs

PEG-DA has been widely used to make cross-linked hydrogels for drug delivery and tissue engineering scaffolding [32, 33].

PEG-DA follows free radical polymerization to form a cross-linked network in the presence of a photoinitiator and UV light. In our studies, we applied PEG-DA (M_n = 575 g/mol) as a cross-linker to improve the stability of electrospun gelatin scaffolds. Short-chained PEG-DA has been found to be less cytocompatible than long-chained PEG-DA presumably due to a higher diffusion rate into the cells [34]. According to the cytotoxicity analysis of PEG-DA (M_n = 575 g/mol) on 3T3-L1 preadipocytes, its IC_{50} was 218 μM (Fig. 1a). Thus, it is important to efficiently cross-link PEG-DA to make the resultant sIPNs cytocompatible.

In the presence of an electron donor such as TEOA, which acts as a co-initiator, eosin Y initiates acrylate polymerization when irradiated. Polymerization occurs as a result of the formation of free radicals originating from TEOA [35]. However, free radicals generated in the polymerization can be a potential cytotoxic source as well. Cross-linking efficiency is affected by the molar ratio of macromonomer to photoinitiator, which in turn, influences cytocompatibility of the resulting sIPNs. Thus, it is important to optimize the ratio of PEG-DA to photoinitiator in the formulation in order to obtain a cytocompatible sIPN-GF formulation. It has been reported that eosin Y (0.005 mM or above) were able to initiate cross-linking of PEG-DA (10%) based on the fractional factorial test which was designed to measure dynamic modulus and swelling ratio for hydrogels [36]. The report also indicated that eosin Y (0.01 mM) and TEOA (0.1%) were cytocompatible for encapsulation of human mesenchymal stem cells (hMSCs) with 88.4% cell viability; whereas eosin Y (0.1 mM) and TEOA (0.75%) were not highly cytocompatible for encapsulation of hMSCs with only 68.8% cell viability [36]. These results indicate extra amount of eosin Y and TEOA could be cytotoxic to the cells. In this work, we tested cytocompatibility of sIPN-GF1, 2, 3, 4 cross-linked with various concentrations of PEG-DA (1, 2, 5 and 10% *w/v*) in the presence of eosin Y photoinitiator solution (5% *v/v*). As expected, GF2 treated with eosin Y photoinitiator solution only did not cause cytotoxicity to 3T3-L1 preadipocytes (Fig. 1b). Neither did sIPN-GF1. However, sIPN-GF cytocompatibility reduced significantly as PEG-DA concentration increased to 2%. It caused 80% cell death. A further increase in PEG-DA concentration led to a more pronounced cytotoxic effect, presumably due to inefficient cross-linking of PEG-DA. Furthermore, we cross-linked PEG-DA (1–10%) using the eosin Y photoinitiator solution (5% eosin Y and 40% TEOA), which was equivalent to 0.77 μM eosin Y. The ratio of PEG-DA (1%) to eosin Y (0.77 μM) was closed to the ratio of PEG-DA (10%) to eosin Y (0.01 mM) as reported, indicating a sufficient cross-linking of PEG-DA initiated by eosin Y photoinitiating system in the sIPN-GF1 formulation.

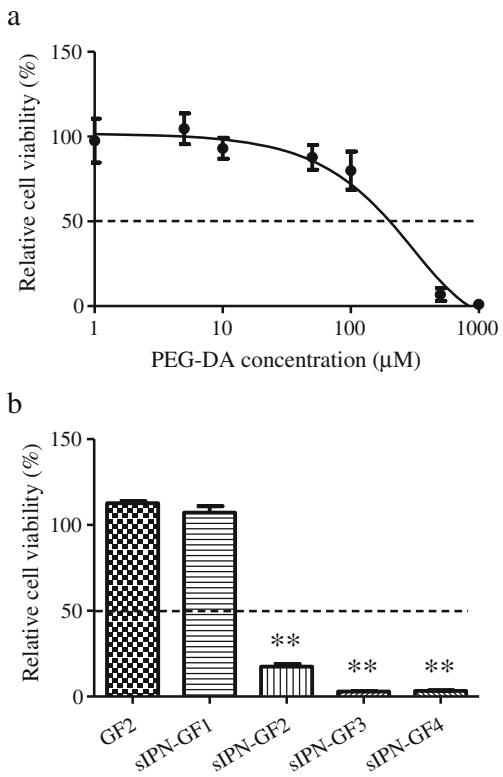

Fig. 1 Cytocompatibility assessment. (**a**) Dose-dependent cytotoxicity of PEG-DA. (**b**) Effects of ratios of PEG-DA to eosin Y photoinitiator solution on the scaffold cytocompatibility. The dots/bars and error bars are mean ± SD. ** $P < 0.01$ *versus* NA treatment.

Cross-linking helps improve structural stability of electrospun gelatin fibers. The cross-linking process resulted in multifold enhancement in the mechanical properties. Following cross-linking, peak load, peak stress, modulus, strain at break and energy at break of GF1 were increased by 6.5, 7.9, 5.0, 2.4 and 17.1 fold, respectively (Table II). Nevertheless, cross-linking process affects structural features of the resulting scaffolds. GF1 consists of fine continuous fibers. However, the cross-linked GF1 (*i.e.*, sIPN-GF1) becomes less porous due to fiber swelling and fusion during the cross-linking reaction (Fig. 2a-b).

Degradation kinetics of sIPN-GFs

The *in vitro* degradation profiles of sIPN-GFs and GFs best fit one phase decay model (Fig. 3a–b). GFs (*e.g.*, GF1) readily dissolve in DMEM in 30 min and are not suitable for controlled drug release. Similar to GF1, GF3 exhibited rapid degradation kinetics, because PEG-DA alone was unable to undergo the cross-linking reaction. In contrast, sIPN-GFs have gained improved stability. sIPN-GFs cross-linked with PEG-DA (1% *w/v*) in the presence of increasing concentrations of eosin Y photoinitiator solution (0–10% *v/v*) have longer scaffold degradation half-lives ($t_{1/2}$) and lower degradation rate constants (K_d) (Fig. 3a, Table III). sIPN-GF5 degraded completely in 60 min. sIPN-GF1 degraded more slowly and still kept 24% of its original mass at 120 min. sIPN-

Table II Mechanical properties of GF1 and sIPN-GF1

	n #	Fiber Diameter (μm)	Thickness (in)	Peak Load (N)	Peak Stress (MPa)	Modulus (MPa)	Strain At Break (mm/mm)	Energy To Break (N*mm)
GF1	18	3.2 ± 1.2	0.018 ± 0.004	2.4 ± 1.2	2.1 ± 1.1	136 ± 53	0.02 ± 0.01	0.23 ± 0.17
sIPN-GF1	12	4.9 ± 1.5 **	0.015 ± 0.002 **	15.7 ± 1.4 **	16.1 ± 1.5 **	677 ± 75 **	0.05 ± 0.01 **	3.88 ± 1.18 **

The data represents mean ± SD. ** $P < 0.01$ compared with GF1

GF6 has the lowest degradation rate and only lost approximately 25% mass at 120 min. The degradation kinetics of sIPN-GF1 in SSF was similar to that of sIPN-GF1 in DMEM. Its $t_{1/2}$ and K_d in SSF were 43.5 min and 0.016, respectively (Fig. 3b).

Microstructural changes of sIPNs during the degradation were also examined using SEM. The changes in structural morphology were concurrent with its degradation kinetics (Fig. 3a). Immediately following incubation, sIPN-GF1 began to lose fiber structures and became more porous. During the first hour of degradation, the scaffold still maintained some fibers. However, at 2 h, sIPN-GF1 completely lost its defined three-dimensional structure and broke into pieces (Fig. 2c–f).

Insulin Release Kinetics and Bioactivity

As shown in Fig. 4, GIF released insulin rapidly due to unstable scaffold integrity. About 86% insulin was released

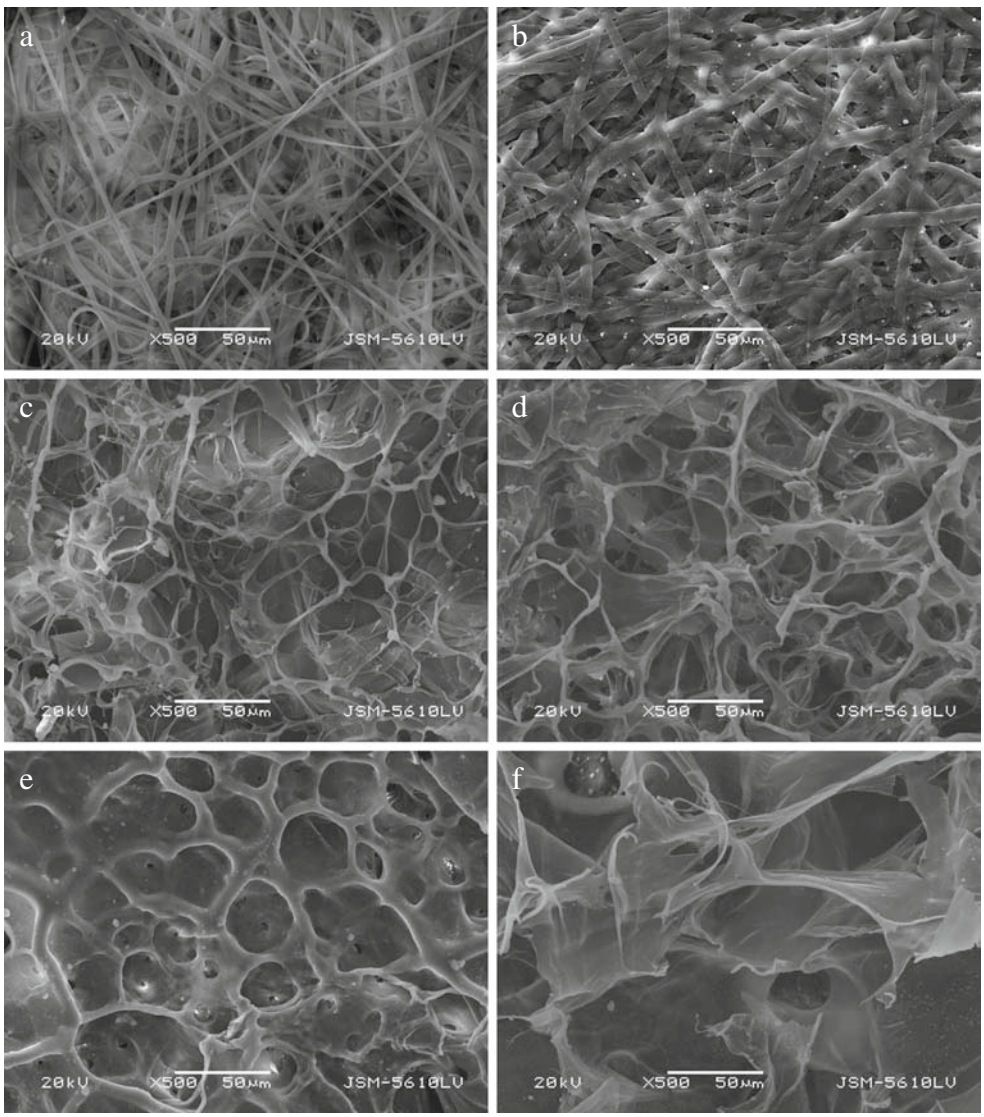

Fig. 2 Representative SEM images of GFs and sIPN-GFs. GF1 (**a**) and sIPN-GF1 (**b**) as well as sIPN-GF1 after 15 min of degradation (**c**), 30 min of degradation (**d**), 60 min of degradation (**e**) and 120 min of degradation (**f**) was observed by SEM. *Bars*: 50 μm.

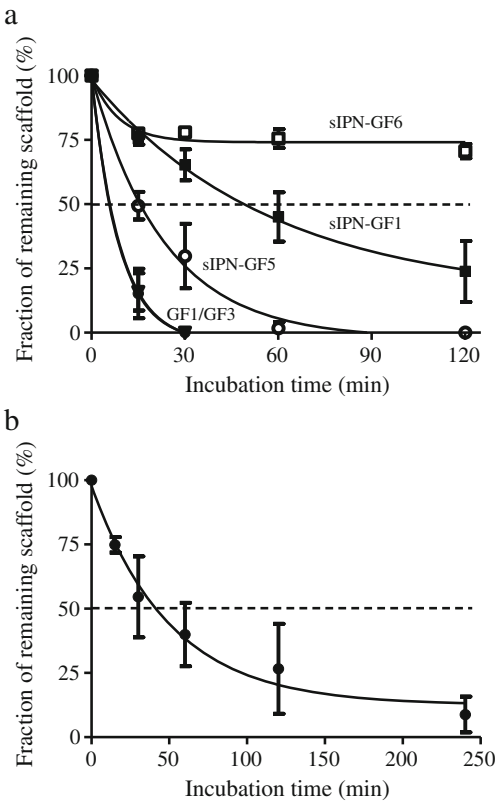

Fig. 3 *In vitro* degradation kinetics of GFs and sIPN-GFs in DMEM (**a**). *In vitro* degradation of sIPN-GF1 in SSF (**b**). The *dots* and *error bars* are mean ± SD.

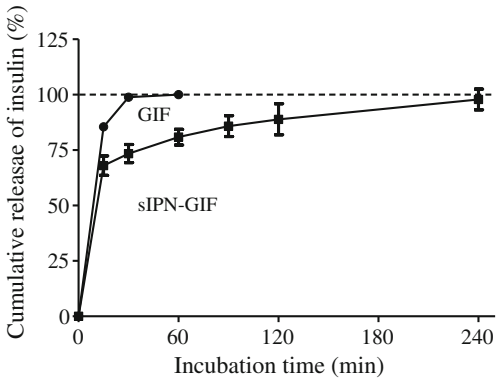

Fig. 4 *In vitro* insulin release kinetics. GF1 formulation was used to prepare GIF, and sIPN-GF1 formulation was used to prepare sIPN-GIF. The *dots* and *error bars* are mean ± SD.

within 15 min, and 100% insulin was completely released within 30 min (Fig. 4). The actual loading density of insulin was determined to be 3.25 mg/g, lower than the feeding ratio of insulin to gelatin, *i.e.*, 5 mg/g, presumably due to attrition in electrospinning. In general, 1 unit of insulin is equivalent to approximately 36 μg of insulin, which can dispose 12–15 g of carbohydrate. Our sIPN-GIF formulation contained 90 units per 1 g of gelatin scaffold.

Insulin release was extended by sIPN-GIF. Insulin was completely released at 4 h (Fig. 4). A burst release of nearly 70% of insulin from sIPN-GIF was observed within 15 min of incubation. This observation may be attributed to two major factors: rapid scaffold degradation and high insulin diffusion. The scaffold remained stable up to 2 h, enabling an extended insulin release from sIPN-GIF. As a result, 100% insulin release was extended to 4 h as a result of slower degradation

Table III Degradation properties of GF and sIPN-GF in DMEM

Scaffold	$t_{1/2}$ (min)	K_d
GF1	6	0.115
GF3	5.9	0.118
sIPN-GF1	49	0.014
sIPN-GF5	15.7	0.044
sIPN-GF6	–	–

$t_{1/2}$, degradation half-life; K_d, degradation rate constant; -, undetermined in the given time period

of sIPN-GIF. Theoretically, increase of both PEG-DA and eosin Y may increase cross-link density, thus reducing burst release and achieving a longer insulin release.

To determine if the bioactivity of insulin loaded in sIPN-GIF remained following electrospinning and cross-linking, we evaluated phosphorylation of AKT at serine-473 in 3T3-L1 preadipocytes treated with insulin released from GIF. Insulin triggers intracellular signal transduction by binding to the extracellular portion of the alpha subunits of the insulin receptor. After binding occurs, it induces a conformational change of the insulin receptor, activating the kinase domain on the intracellular portion of the beta subunits. The activated kinase phosphorylates IRS-1 protein activates phosphoinositide-3 kinase (PI3K), which then stimulates phosphorylation of AKT (protein kinase B, PKB) [37]. AKT phosphorylation level was increased by 6.2-fold in insulin-treated group (20 μg) as compared with no treatment group (NA). 20 mg of GIF was dissolved in 5 mg of cell culture media to yield a concentration of 4 mg/ml. Because the actual loading density of insulin in GIF was 3.25 mg/g, the insulin concentration in the released media of GIF was 13 μg/ml. Our results showed that AKT phosphorylation level was significantly increased by 6.3-fold in the cells incubated with 2 ml of GIF-based insulin release medium (containing 26 μg of insulin), suggesting most insulin retained bioactivity following electrospinning (Fig. 5a–b). We further examined the bioactivity of insulin released from sIPN-GIF after cross-linking. We found that AKT phosphorylation level increased over a time course of 120 min in a time-dependent manner, which corresponded to cumulative insulin release kinetics (Fig. 5c–d). Insulin released from sIPN-GIF for a period of 120 min was able to induce AKT phosphorylation to the same level as it from GIF for a period of 30 min. According to the insulin release kinetics (Fig. 4), about 89% of insulin was released from sIPN-GIF in 120 min. Thus, 20 mg of sIPN-GIF degraded in 5 ml of cell culture media for 120 min, yielding 11.7 μg/ml of insulin in solution. The cells were treated with 2 ml of sIPN-GIF 120 min-release media (yielding 23.4 μg of

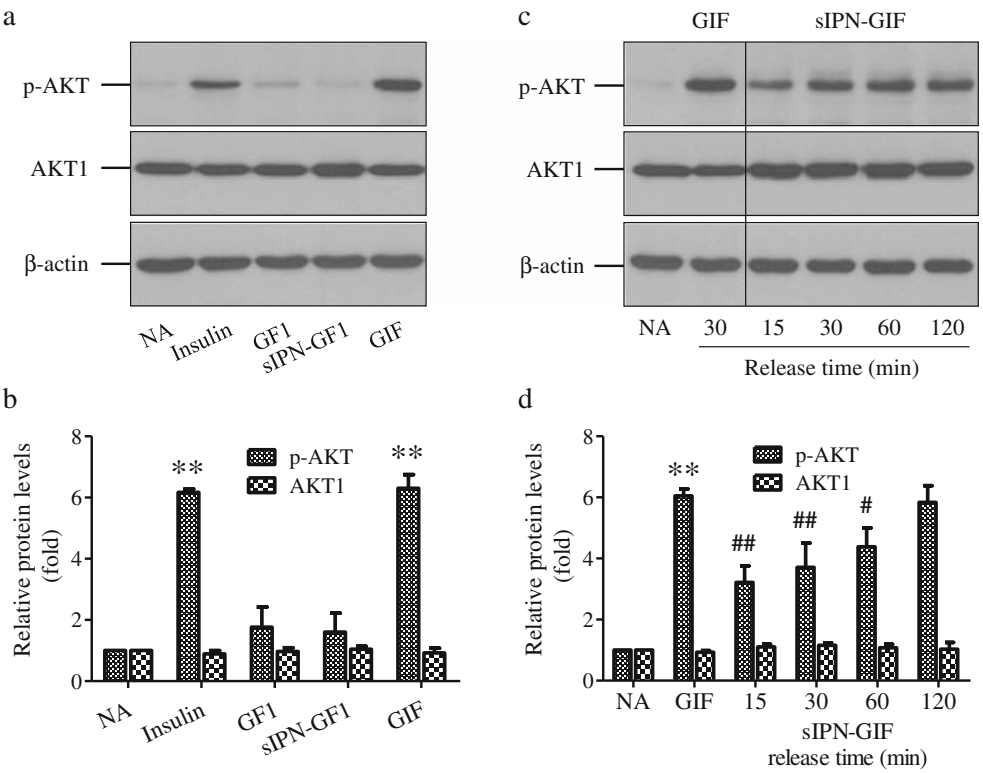

Fig. 5 Western blot analysis of intracellular AKT activity in response to the fabricated scaffolds. The p-AKT and AKT1 levels were analyzed by Western blot analysis (**a**, **c**). Each positive band was normalized to β-actin and was quantified by NIH ImageJ (**b**, **d**). The data represents typical one of three experiments. The *bars* and *error bars* are mean ± SD. $^{**}P < 0.01$ *versus* NA treatment; $\#P < 0.05$ and $\#\#P < 0.01$ *versus* GIF treatment.

insulin) exhibited similar AKT activity as the cells treated with free insulin (20 μg) or GIF (26 μg of insulin), with no statistical difference, indicating the insulin receptor or insulin signaling pathway might be saturated in these preadipocytes. Taken together, our results illustrated most insulin can retain its activity after the electrospinning and crosslinking process.

To further confirm these results, we evaluated 3T3-L1 preadipocytes differentiation in sIPN-GIF 120 min-release media. As expected, no lipid inclusion was apparent in sIPN-GF and negative control treatment groups, whereas several lipid inclusions were observed in sIPN-GIF (yielding 23.4 μg of insulin) and free insulin (20 μg) treatment groups, indicating a successful adipocyte differentiation (Fig. 6).

In Vitro Transport of Insulin Across Buccal Mucosa

A vertical Franz diffusion cell mounted with a porcine buccal mucosal membrane was used as an *in vitro* model to test the permeability of insulin across the buccal mucosa. Diffusion rates of insulin loaded in sIPN-GIF (2.5 mg) and free insulin (8.125 μg) across the porcine buccal mucosa were determined. All the cumulative flux curves were displayed in a linear range during the first 2 h, indicating a steady state transport of insulin *via* the paracellular route (Fig. 7). Permeability was then calculated from the linear range of the cumulative flux curves. The permeability of insulin from sIPN-GIF was determined to be 1.00×10^{-7} cm/s, whereas the permeability of free insulin was 7.67×10^{-8} cm/s. A 30% enhancement of permeability was achieved by the use of sIPN-GIF. Further analysis indicated that 22.3% insulin loaded in sIPN-GIF permeated through the porcine buccal mucosa in 4 h.

DISCUSSION

In this work, we investigated electrospun fibers for transbuccal delivery of insulin. It is important to prove that insulin remains bioactive after the electrospinning and cross-linking process. Electrospinning and UV light-initiated cross-linking may alter the three-dimensional structure of proteins, causing protein denaturation. To date, a few studies have reported biological proteins can be co-electrospun with polymers without losing their bioactivity. For instance, purified adipose tissue-derived extracellular matrix (At-ECM) can be electrospun alone or co-electrospun with polydioxanone (PDO). The resultant scaffold forms a basement membrane-rich tissue engineering matrix that is capable of supporting adipose stem cells [38]. In this work, we demonstrated that most insulin remains bioactive after electrospinning as GIF was able to trigger intracellular AKT phosphorylation. sIPN-GIF was able to trigger intracellular AKT phosphorylation in a time-dependent manner, indicating insulin remains bioactive after fiber cross-linking. It was noticed that this AKT phosphorylation kinetics of sIPN-

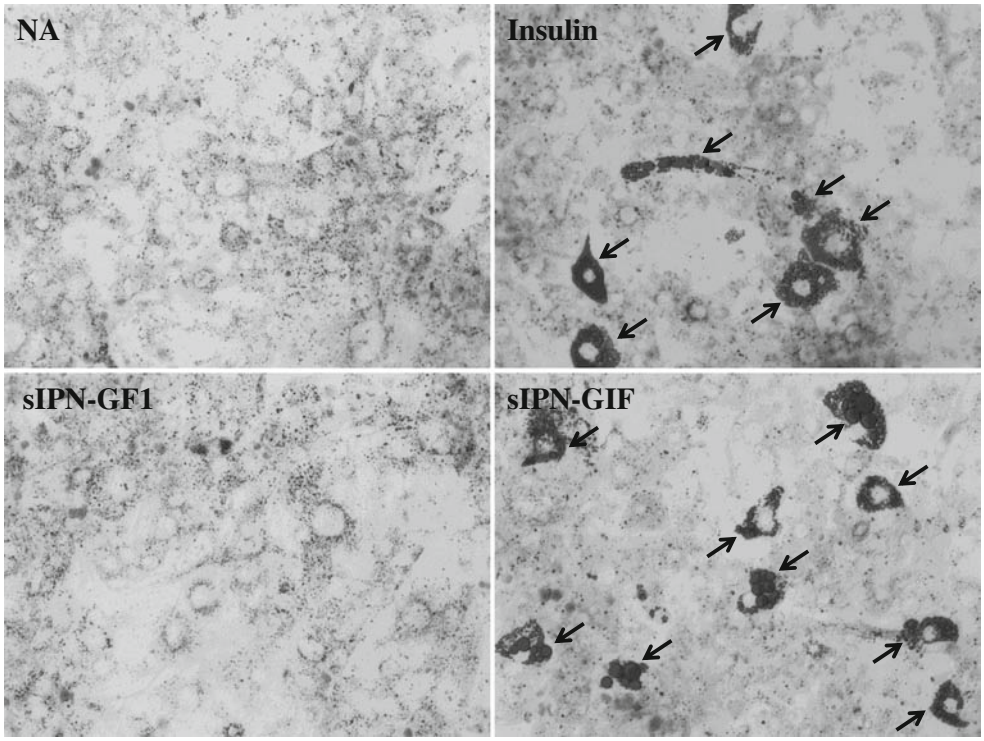

Fig. 6 Oil red O staining of 3T3-L1 preadipocytes following insulin, sIPN-GF1 or sIPN-GIF treatment. *Arrows* indicate stained lipid inclusions. Original magnification × 400.

GIF was consistent with the degradation kinetics of sIPN-GF1. The differentiation of 3T3-L1 preadipocytes was also evaluated in regard to the insulin released from sIPN-GIF. Furthermore, our results showed sIPN-GIF could successfully induce 3T3-L1 preadipocytes differentiation. Together, from biochemistry and biology aspects, we confirmed that most insulin in sIPN-GIF retains bioactivity after co-electrospinning and cross-linking.

Transport of hydrophilic molecules across the buccal membrane generally occurs *via* a paracellular route that is driven by passive diffusion [31]. Due to good biodegradability, moderate stiffness and satisfactory tissue adhesiveness properties, gelatin/PEG sIPN have been investigated for delivery of biomacromolecules and controlled release [39, 40]. It has been reported that mucoadhesive hydrogels can open up the cell junctions of the stratified squamous epithelium by dehydrating the cells as they swell, thus increasing the permeability of the drug [2]. In addition, direct surface contact between the gels and the mucosa could result in localization of drug at the mucosal surface, hereby facilitating buccal transport of the drug. Based on our understanding of these mechanisms, a gelatin/PEG sIPN was developed to enhance transbuccal delivery of dendritic nanoparticles using an *in vitro* model [31]. Although PEG-only hydrogel has been shown to enhance transbuccal delivery of dendritic nanoparticles, the lack of mucosal adhesiveness makes PEG-only hydrogel unsuitable for buccal administration [31]. Prior studies have been conducted to examine transbuccal delivery of insulin [19, 20, 41, 42], but none of them was based on electrospun fiber formulations. Soybean-lecithin (SLT) emulsion with sodium deoxycholic acid was found to enhance insulin diffusion across the porcine mucosal tissue, and the buccal permeability of insulin in SLT was 1.32×10^{-7} cm/s [41]. Our results showed the buccal permeability of insulin in sIPN-GIF was 1.00×10^{-7} cm/s, which was similar to insulin permeability achieved by SLT. It is advantageous of using sIPN-GIF because it can localize insulin to the buccal mucosal site and enable sustained release. Permeation enhancers, such as sodium glycodeoxycholate (NaGDC) can be incorporated into

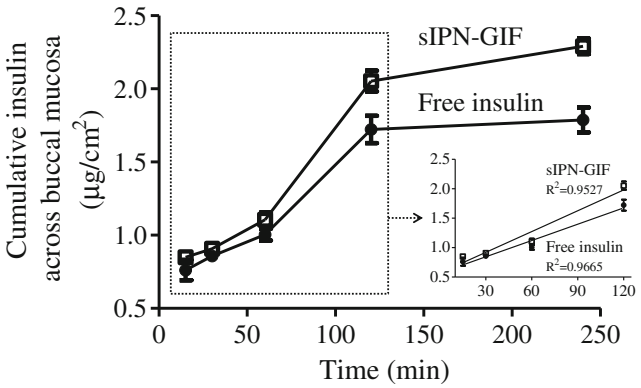

Fig. 7 Transport of insulin across the porcine buccal mucosa from sIPN-GIF and free insulin. Diffusion rate of insulin across porcine buccal mucosa from sIPN-GIF and free insulin. The *dots* and *error bars* are mean ± SD.

sIPN-GIF to enhance transbuccal permeability of insulin [31] and will be explored in future work.

CONCLUSIONS

sIPN co-electrospun gelatin/insulin fiber formulation with good cytocompatibility and moderate degradation was successfully fabricated. Insulin release from the scaffold was extended, and the released insulin has proven to be bioactive by triggering AKT phosphorylation in 3T3-L1 preadipocytes and inducing preadipocyte differentiation. sIPN-GIF formulation resulted in enhanced transbuccal transport of insulin. Taken together, sIPN-GIF has been shown as a potential formulation for transbuccal delivery of insulin.

ACKNOWLEDGMENTS AND DISCLOSURES

This work was supported, in part, by the National Science Foundation CAREER award (CBET0954957). The authors acknowledge the technical advice of the Franz diffusion cell system provided by Dr. Quan Yuan (Department of Internal Medicine, Virginia Commonwealth University).

REFERENCES

1. Golden SH, Sapir T. Methods for insulin delivery and glucose monitoring in diabetes: summary of a comparative effectiveness review. J Manag Care Pharm. 2012;18(6 Suppl):S1–17.
2. Salamat-Miller N, Chittchang M, Johnston TP. The use of mucoadhesive polymers in buccal drug delivery. Adv Drug Deliv Rev. 2005;57(11):1666–91.
3. Chen MC, Sonaje K, Chen KJ, Sung HW. A review of the prospects for polymeric nanoparticle platforms in oral insulin delivery. Biomaterials. 2011;32(36):9826–38.
4. Soares S, Costa A, Sarmento B. Novel non-invasive methods of insulin delivery. Expert Opin Drug Deliv. 2012;9(12):1539–58.
5. el Khafagy S, Morishita M, Onuki Y, Takayama K. Current challenges in non-invasive insulin delivery systems: a comparative review. Adv Drug Deliv Rev. 2007;59(15):1521–46.
6. Sonia TA, Sharma CP. An overview of natural polymers for oral insulin delivery. Drug Discov Today. 2012;17(13–14):784–92.
7. Cui F, Shi K, Zhang L, Tao A, Kawashima Y. Biodegradable nanoparticles loaded with insulin-phospholipid complex for oral delivery: preparation, in vitro characterization and in vivo evaluation. J Control Release. 2006;114(2):242–50.
8. Cui FD, Tao AJ, Cun DM, Zhang LQ, Shi K. Preparation of insulin loaded PLGA-Hp55 nanoparticles for oral delivery. J Pharm Sci. 2007;96(2):421–7.
9. Li X, Qi J, Xie Y, Zhang X, Hu S, Xu Y, *et al.* Nanoemulsions coated with alginate/chitosan as oral insulin delivery systems: preparation, characterization, and hypoglycemic effect in rats. Int J Nanomedicine. 2013;8:23–32.
10. Oak M, Singh J. Chitosan-zinc-insulin complex incorporated thermosensitive polymer for controlled delivery of basal insulin in vivo. J Control Release. 2012;163(2):145–53.
11. Chalasani KB, Russell-Jones GJ, Yandrapu SK, Diwan PV, Jain SK. A novel vitamin B12-nanosphere conjugate carrier system for peroral delivery of insulin. J Control Release. 2007;117(3):421–9.
12. Krauland AH, Guggi D, Bernkop-Schnürch A. Oral insulin delivery: the potential of thiolated chitosan-insulin tablets on non-diabetic rats. J Control Release. 2004;95(3):547–55.
13. Sonaje K, Lin Y-H, Juang J-H, Wey S-P, Chen C-T, Sung H-W. In vivo evaluation of safety and efficacy of self-assembled nanoparticles for oral insulin delivery. Biomaterials. 2009;30(12):2329–39.
14. Chalasani KB, Russell-Jones GJ, Jain AK, Diwan PV, Jain SK. Effective oral delivery of insulin in animal models using vitamin B12-coated dextran nanoparticles. J Control Release. 2007;122(2):141–50.
15. Liu W, Thomopoulos S, Xia Y. Electrospun nanofibers for regenerative medicine. Adv Healthc Mater. 2012;1(1):10–25.
16. Sudhakar Y, Kuotsu K, Bandyopadhyay AK. Buccal bioadhesive drug delivery–a promising option for orally less efficient drugs. J Control Release. 2006;114(1):15–40.
17. Morishita M, Barichello JM, Takayama K, Chiba Y, Tokiwa S, Nagai T. Pluronic F-127 gels incorporating highly purified unsaturated fatty acids for buccal delivery of insulin. Int J Pharm. 2001;212(2):289–93.
18. Giovino C, Ayensu I, Tetteh J, Boateng JS. Development and characterisation of chitosan films impregnated with insulin loaded PEG-b-PLA nanoparticles (NPs): a potential approach for buccal delivery of macromolecules. Int J Pharm. 2012;428(1–2):143–51.
19. Giovino C, Ayensu I, Tetteh J, Boateng JS. An integrated buccal delivery system combining chitosan films impregnated with peptide loaded PEG-b-PLA nanoparticles. Colloids Surf B: Biointerfaces. 2013;112:9–15.
20. Cui F, He C, He M, Tang C, Yin L, Qian F, *et al.* Preparation and evaluation of chitosan-ethylenediaminetetraacetic acid hydrogel films for the mucoadhesive transbuccal delivery of insulin. J Biomed Mater Res. 2009;89(4):1063–71.
21. Morales JO, Ross AC, McConville JT. Protein-coated nanoparticles embedded in films as delivery platforms. J Pharm Pharmacol. 2013;65(6):827–38.
22. Ayensu I, Mitchell JC, Boateng JS. In vitro characterisation of chitosan based xerogels for potential buccal delivery of proteins. Carbohydr Polym. 2012;89(3):935–41.
23. Sill TJ, von Recum HA. Electrospinning: applications in drug delivery and tissue engineering. Biomaterials. 2008;29(13):1989–2006.
24. Aduba Jr DC, Hammer JA, Yuan Q, Yeudall WA, Bowlin GL, Yang H. Semi-interpenetrating network (sIPN) gelatin nanofiber scaffolds for oral mucosal drug delivery. Acta Biomater. 2013;9(5):6576–84.
25. Desai PN, Yuan Q, Yang H. Synthesis and characterization of photocurable polyamidoamine dendrimer hydrogels as a versatile platform for tissue engineering and drug delivery. Biomacromolecules. 2010;11(3):666–73.
26. Tseng Y-Y, Kao Y-C, Liao J-Y, Chen W-A, Liu S-J. Biodegradable drug-eluting poly[lactic-co-glycol acid] nanofibers for the sustainable delivery of vancomycin to brain tissue: in vitro and in vivo studies. ACS Chem Neurosci. 2013;4(9):1314–21.
27. McClure MJ, Wolfe PS, Simpson DG, Sell SA, Bowlin GL. The use of air-flow impedance to control fiber deposition patterns during electrospinning. Biomaterials. 2012;33(3):771–9.
28. Xu L, Shen S, Ma Y, Kim JK, Rodriguez-Agudo D, Heuman DM, *et al.* 25-Hydroxycholesterol-3-sulfate attenuates inflammatory response via PPARgamma signaling in human THP-1 macrophages. Am J Physiol Endocrinol Metab. 2012;302(7):E788–99.
29. Song DH, Getty-Kaushik L, Tseng E, Simon J, Corkey BE, Wolfe MM. Glucose-dependent insulinotropic polypeptide enhances adipocyte development and glucose uptake in part through Akt activation. Gastroenterology. 2007;133(6):1796–805.
30. Ma Y, Xu L, Rodriguez-Agudo D, Li X, Heuman DM, Hylemon PB, *et al.* 25-Hydroxycholesterol-3-sulfate regulates macrophage lipid

metabolism via the LXR/SREBP-1 signaling pathway. Am J Physiol Endocrinol Metab. 2008;295(6):E1369–79.
31. Yuan Q, Fu Y, Kao WJ, Janigro D, Yang H. Transbuccal delivery of CNS therapeutic nanoparticles: synthesis, characterization, and in vitro permeation studies. ACS Chem Neurosci. 2011;2(11):676–83.
32. Fu Y, Kao WJ. Drug release kinetics and transport mechanisms from semi-interpenetrating networks of gelatin and poly(ethylene glycol) diacrylate. Pharm Res. 2009;26(9):2115–24.
33. Liang Y, Jensen TW, Roy EJ, Cha C, Devolder RJ, Kohman RE, *et al.* Tuning the non-equilibrium state of a drug-encapsulated poly(-ethylene glycol) hydrogel for stem and progenitor cell mobilization. Biomaterials. 2011;32(7):2004–12.
34. Mazzoccoli JP, Feke DL, Baskaran H, Pintauro PN. Mechanical and cell viability properties of crosslinked low- and high-molecular weight poly(ethylene glycol) diacrylate blends. J Biomed Mater Res. 2010;93(2):558–66.
35. Kizilel S, Perez-Luna VH, Teymour F. Photopolymerization of poly(ethylene glycol) diacrylate on eosin-functionalized surfaces. Langmuir. 2004;20(20):8652–8.
36. Bahney CS, Lujan TJ, Hsu CW, Bottlang M, West JL, Johnstone B. Visible light photoinitiation of mesenchymal stem cell-laden bioresponsive hydrogels. Eur Cell Mater. 2011;22:43–55. discussion 55.
37. Jiang ZY, Zhou QL, Coleman KA, Chouinard M, Boese Q, Czech MP. Insulin signaling through Akt/protein kinase B analyzed by small interfering RNA-mediated gene silencing. Proc Natl Acad Sci U S A. 2003;100(13):7569–74.
38. Francis MP, Sachs PC, Madurantakam PA, Sell SA, Elmore LW, Bowlin GL, *et al.* Electrospinning adipose tissue-derived extracellular matrix for adipose stem cell culture. J Biomed Mater Res. 2012;100(7):1716–24.
39. Burmania JA, Stevens KR, Kao WJ. Cell interaction with protein-loaded interpenetrating networks containing modified gelatin and poly(ethylene glycol) diacrylate. Biomaterials. 2003;24(22):3921–30.
40. Zilinski JL, Kao WJ. Tissue adhesiveness and host response of in situ photopolymerizable interpenetrating networks containing methylprednisolone acetate. J Biomed Mater Res. 2004;68(2):392–400.
41. Tian W, Hu Q, Xu Y, Xu Y. Effect of soybean-lecithin as an enhancer of buccal mucosa absorption of insulin. Biomed Mater Eng. 2012;22(1–3):171–8.
42. Xu HB, Huang KX, Zhu YS, Gao QH, Wu QZ, Tian WQ, *et al.* Hypoglycaemic effect of a novel insulin buccal formulation on rabbits. Pharmacol Res. 2002;46(5):459–67.